High-Aspect-Ratio Structures for MEMS

Stella W. Pang

Many microelectromechanical systems (MEMS) use the changing capacitance of movable parallel plates to drive and sense motion.[1–3] An increase in this capacitance improves the performance of these micromechanical structures by means of increased electromechanical coupling for lower driving voltages and increased sensitivity of the micromechanical motion. This means that a high-aspect-ratio trench etched with large depth or small gaps is desirable because it provides increased capacitance. In addition, deep trenches allow thicker devices to be fabricated, thus increasing mass, which is advantageous for inertial sensing applications. From the mechanical point of view, having a larger thickness associated with high-aspect-ratio structures also increases the mechanical stability of the released features and avoids stress-related bending.[4]

These high-aspect-ratio structures are often formed by etching or electroplating. Dry etching has been developed for the patterning of high-aspect-ratio structures. Since directional ions are generated in the plasma, dry etching can produce anisotropic profiles by controlling the density, energy, and distribution of the reactive species in the discharge. Typically, high-density plasma sources such as electron cyclotron resonance or inductively coupled plasma are used with separate power sources to generate the plasma and bias the wafer.[5,6] These plasma sources have the advantages of providing nearly independent control of ion density and ion energy for improved etch characteristics, as well as providing dense plasmas for high etch rates and throughput.

Often, fluorine-containing gases are used to dry-etch high-aspect-ratio deep trenches.[7,8] Because fluorine tends to etch Si isotropically, polymer passivation of the side walls is needed to prevent undercutting and allow etching in the vertical direction.[9] This technique has the advantages of high etch rates and high selectivity to etch masks. However, roughness can form along the side walls due to cycling and passivation effects, and the polymer passivation may prevent the formation of narrow trenches with a high aspect ratio.

An alternative—and simpler—technique for etching high-aspect-ratio Si structures is to use Cl_2 chemistry.[10–12] No passivation is needed, as Cl_2 etching is an ion-assisted process and it tends to be anisotropic. The simpler process, without passivation or switching cycles, makes Cl_2 etching easier to control and more reproducible. Smooth side walls can be obtained because the etch and deposition cycles create no surface roughness. It is especially useful for the etching of trenches with submicrometer dimensions, whereas the need for passivation using fluorine chemistry often limits the width of the trenches that can be patterned. The potential drawbacks of Cl_2 etching of Si are a slower etch rate and lower etch selectivity to mask.

When microsensors with high-aspect-ratio structures are etched, it is essential to maintain a constant etch rate and profile for trenches with different widths in order to ensure identical etch depths for uniform device characteristics. Often, aspect-ratio-dependent etching is observed as a result of the restricted transport of etch species and etch products. For trenches with higher aspect ratios, the average etch rate decreases. Etching at lower pressure or higher ion energy reduces scattering and keeps the reactive species more directional, which minimizes the variations of etch rates with aspect ratio. By applying the optimized etch conditions, uniform etching of high-aspect-ratio microstructures in Si can be achieved.

Figure 1 shows a laterally driven Si micromirror fabricated by the deep-etch–shallow-diffusion process.[13,14] The Si micromirror and microresonator are 50 μm thick, with 2-μm-wide interdigitated comb fingers; the gaps between the comb electrodes are 3 μm. The vertical micromirror is supported by 3-μm-wide, 800-μm-long folded suspension beams. The dry-etching technology developed for high-aspect-ratio microstructures allows large numbers of tall and narrow fingers with small gaps to be formed for large electrostatic force at low voltage to reduce power consumption. It is also advantageous to have narrow suspension beams with large beam thickness, since the beam rigidity

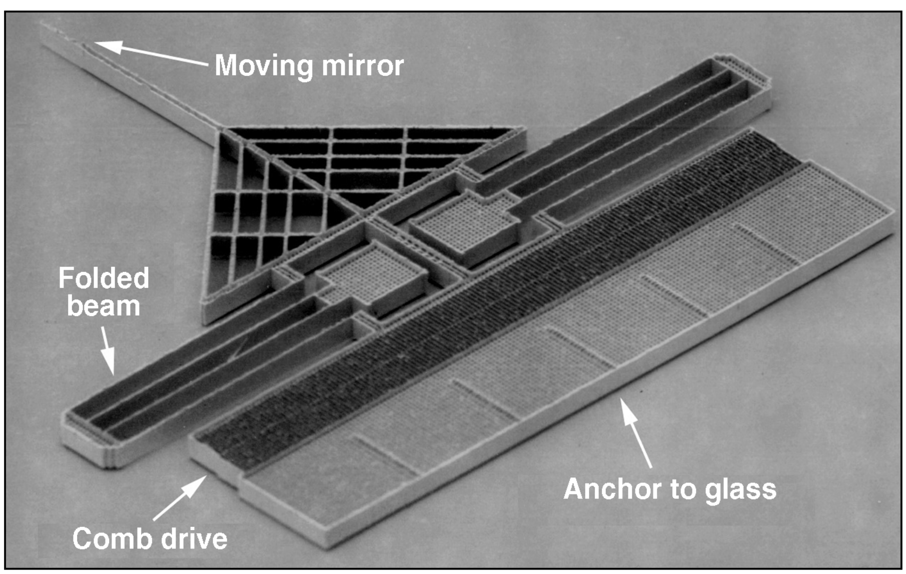

Figure 1. Laterally driven Si micromirror 50 μm thick, with 3-μm-wide folded suspension beams, fabricated by the deep-etch–shallow-diffusion process.

along the vertical direction is increased while remaining very compliant along the lateral direction. This ensures that during optical switching, stiffeners at the ends of these long folded beams are not in contact with the glass substrate due to gravity. These vertical micromirrors supported by folded beams are actuated by the electrostatic comb drives. With the large beam thickness, small gaps for the comb drives, and large number of fingers, only a 30-V dc bias is required for a mirror movement of 30 μm. These high-aspect-ratio, vertical micromirrors fabricated by bulk micromachining can be applied as optical switches for communications networks. (For more on applications of MEMS micromirrors, see the article by Hornbeck in this issue.)

References

1. W.C. Tang, T.-C.H. Nguyen, M.W. Judy, and R.T. Howe, *Sens. Actuators, A* **21–23** (1990) p. 328.
2. J.M. Bustillo, R.T. Howe, and R.S. Muller, in *Proc. IEEE* **86** (1998) p. 1552.
3. J.W. Weigold, W.H. Juan, and S.W. Pang, *J. Electrochem. Soc.* **145** (1998) p. 1767.
4. J.W. Weigold, W.H. Juan, S.W. Pang, and J.T. Borenstein, *J. Vac. Sci. Technol., B* **17** (1999) p. 1336.
5. W.H. Juan and S.W. Pang, *J. Vac. Sci. Technol., B* **12** (1994) p. 422.
6. W.H. Juan and S.W. Pang, *IEEE/ASME J. MEMS* **5** (1996) p. 18.
7. M.B. Stern and S.S. Medeiros, *J. Vac. Sci. Technol., B* **10** (1992) p. 2520.
8. E.H. Klaassen, K. Petersen, J.M. Noworolski, J. Logam, N.I. Maluf, J. Brown, C. Storment, W. McCulley, and G.T.A. Kovacs, *Sens. Actuators, A* **52** (1996) p. 132.
9. V.A. Yunkin, D. Fischer, and E. Voges, *Microelectron. Eng.* **23** (1994) p. 373.
10. W.H. Juan and S.W. Pang, *J. Vac. Sci. Technol., A* **14** (1996) p. 1189.
11. J.W. Weigold and S.W. Pang, *IEEE/ASME J. MEMS* **7** (1998) p. 201.
12. J.W. Weigold, A.-C. Wong, C.T.-C. Nguyen, and S.W. Pang, *IEEE/ASME J. MEMS* **8** (1999) p. 221.
13. W.H. Juan and S.W. Pang, *J. Vac. Sci. Technol., B* **14** (1996) p. 4080.
14. W.H. Juan and S.W. Pang, *IEEE/ASME J. MEMS* **7** (1998) p. 207. □